

Perturbation effect of BN-bonds on tetracyclo[8,2,0,02,5,06,9]dodeca-1,3,5,7,9,11-hexaene and some subunits of it – A DFT treatment

Lemi Türker

Department of Chemistry, Middle East Technical University, Üniversiteler, Eskişehir Yolu No: 1, 06800 Çankaya/Ankara, Turkey
e-mail: lturker@gmail.com; lturker@metu.edu.tr

Abstract

A tetracyclo compound having 12 carbons (tetracyclo[8,2,0,02,5,06,9]dodeca-1,3,5,7,9,11-hexaene) was subjected to perturbations by inserting 1-3 B-N covalent-bonds into its π -system allowing the arouse of various isomers. Presently, those various BN-bond having structures have been investigated thoroughly within the constraints of density functional theory at the level of B3LYP/6-311++G(d,p). The collected data have revealed that the optimized structures of them have exothermic heats of formation and favorable Gibbs free energy of formation values. They are thermally favored and electronically stable at the standard states. Various structural and quantum chemical data have been collected and discussed, including UV-VIS spectra. Some structures are found to be isospectral isomers.

1. Introduction

Although annulenes by definition are monocyclic π -conjugated systems there exist some structures, like corannulene, which have many rings but their peripheral skeleton resemble an annulene. In that respect structure-1 might be an interesting system itself. However, its BN-bond(s) embedded perturbed forms apt to some quire behavior.

The tetracyclo compound having 12 carbons, namely tetracyclo[8,2,0,02,5,06,9]dodeca-1,3,5,7,9,11-hexaene (structure-1) is an even alternant system [1]. Figure 1 shows two resonance structures of structure-1.

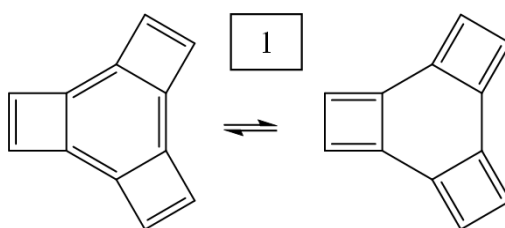
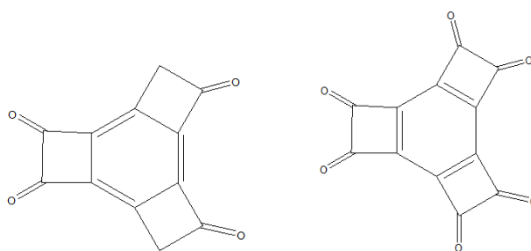


Figure 1. Two resonance forms of structure-1.

Some oxostructures which topologically resemble structure-1 have been mentioned in the literature [2-4].



The B-N covalent-bond-embedded π -conjugated moieties are suitable to act as electron-rich units in order to construct electron-donor materials owing to their high-lying energy levels, good backbone co-planarity, and high hole mobility. However, their absorption bands should be further broadened to lower energy (600–800 nm) to enhance the light harvesting ability [2].

The first wave of BN-heteroarene research began in the late 1950s with Dewar's studies of polycyclic derivatives of BN-naphthalenes, phenanthrene, and tetraphenes. The early syntheses of these compounds often employed harsh conditions and afforded products in low overall yields [5]. The photoisomerization [6] and Diels-Alder cycloaddition [7] of 1,2-azaborines to form heteroatom-substituted cyclobutane and cyclohexane derivatives, respectively, represent promising initial leads toward this development. Recently, developments in azaborine chemistry facilitated construction/insertion of BN bond(s) [8,9].

2. Method of Calculations

In the present study, all the initial optimizations of the structures leading to energy minima have been achieved first by using MM2 method which is then followed by semi empirical PM3 self consistent fields molecular orbital method [10-12]. Afterwards, the structure optimizations have been achieved within the framework of Hartree-Fock and finally by using density functional theory (DFT) at the level of B3LYP/6-311++G(d,p) [13,14]. Note that the exchange term of B3LYP consists of hybrid Hartree-Fock and local spin density (LSD) exchange functions with Becke's gradient correlation to LSD exchange [15]. The correlation term of B3LYP consists of the Vosko, Wilk, Nusair (VWN3) local correlation functional [16] and Lee, Yang, Parr (LYP) correlation correction functional [17]. In the present study, the normal mode analysis for each structure yielded no imaginary frequencies for the $3N-6$ vibrational degrees of freedom, where N is the number of atoms in the system. This search has indicated that the structure of each molecule considered corresponds to at least a local minimum on the potential energy surface. Furthermore, all the bond lengths have been thoroughly searched in order to find out whether any bond cleavages occurred or not during the geometry optimization process. All these computations were performed by using SPARTAN 06 program [18].

3. Results and Discussion

Tetracyclo[8,2,0,02,5,06,9]dodeca-1,3,5,7,9,11-hexaene (Figure 1) is an even alternant structure having a 6-membered core which is fused with three 4-membered cyclobutadiene-like flanked subunits. Figure 2 shows the optimized structure of the tetracyclo compound considered as the parent carbocyclic structure (Figure 1). All the other structures presently considered are either BN bond having (perturbed) species originating from 1 or some perturbed subunits of it.



Figure 2. Optimized structure of the tetracyclo compound considered (two different views).

Figure 3 displays regioisomers of the three BN-bond having tetracyclo molecule derived from structure-1. Note that isomer-2 possesses C₃-axis of symmetry whereas 2' does not. Note the different sequence of boron and nitrogen atoms in the isomers shown in Figure 3.

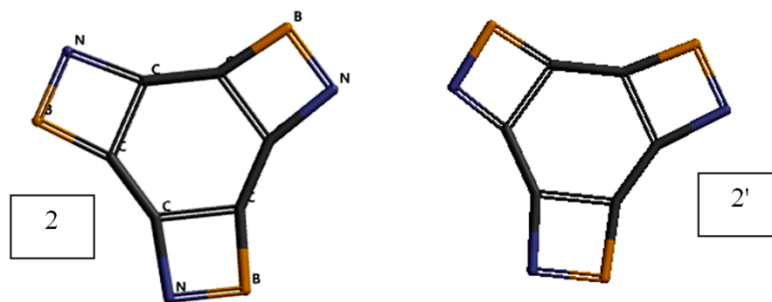


Figure 3. Structures of BN-bond having tetracyclo species derived from structure-1 (not optimized).

Figure 4 shows some optimized subunits of structures-2 and 2'. Note that substructure-4 possesses nitrogen and boron atoms located around the periphery (some sorts of) alternatingly whereas in substructures-5 and -6 this is not the case. The perturbed structures are derived from structure-1 by replacing C=C bonds of 4-membered rings by B=N bonds (or by means of series of centric perturbations [1]).

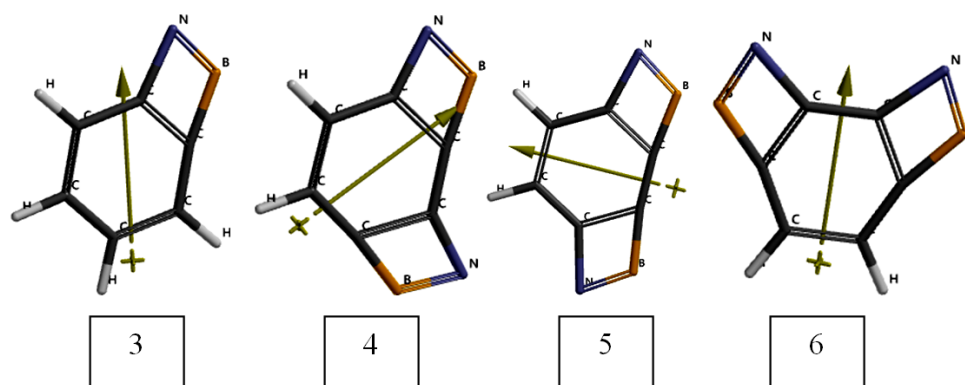
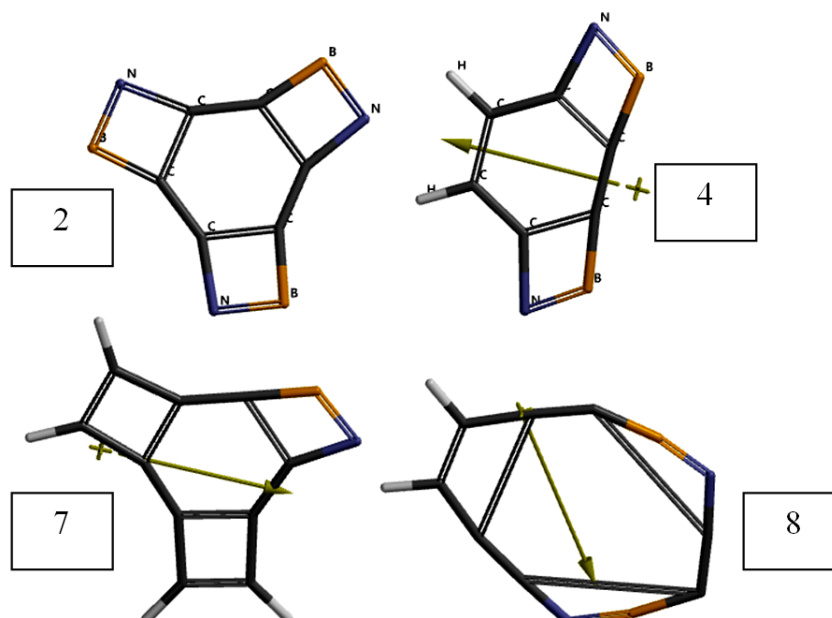


Figure 4. Some optimized subunits of structure-2 and 2'.

Figure 5 shows structure-2 (not optimized) and nine of the optimized perturbed cyclic structures derived from structure-1. Note that structures 8-13 are the optimized structures obtained from structure-2 or 2' which have more than one BN bonds. For structures-8, 10 and 12 the optimization process yielded some other structures (9, 11 and 13, respectively) which are considered below in detailed.



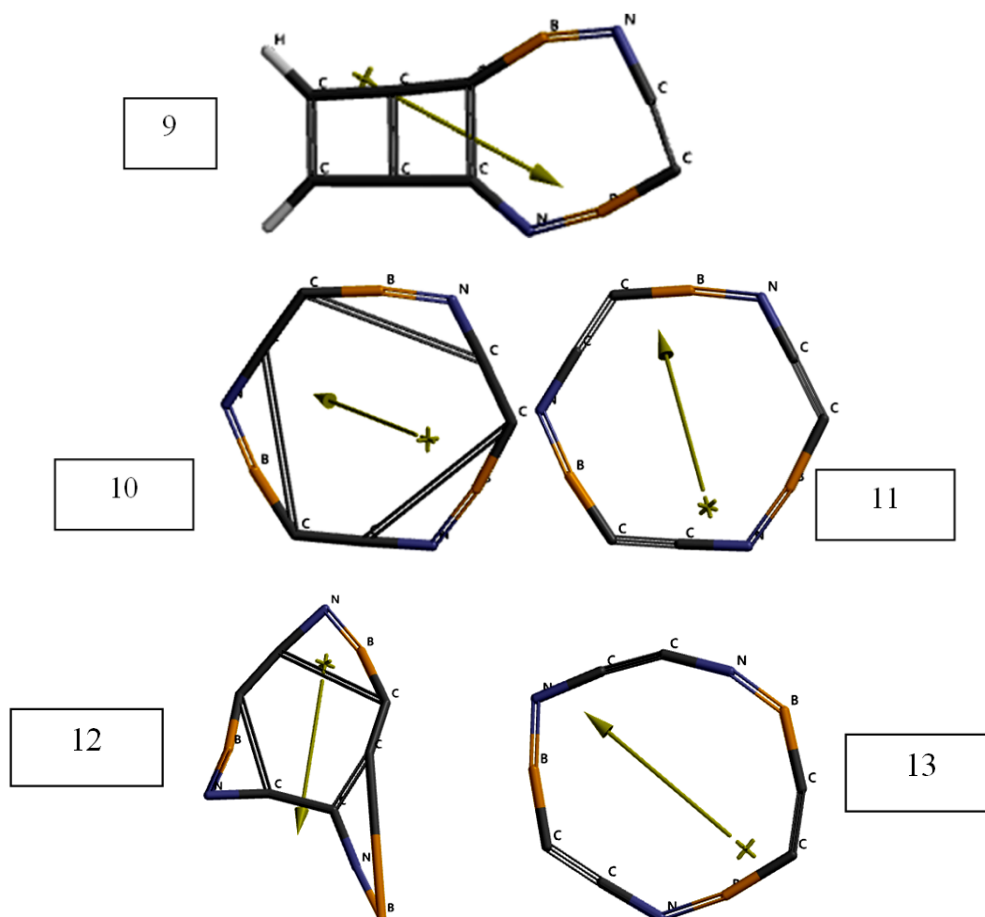


Figure 5. Optimized perturbed tetracyclo structures derived from structure-1.

Figures 6 and 7 display ESP charges on atoms of various structures. Note that the ESP charges are obtained by the program which uses a numerical method that generates charges, thus reproducing the electrostatic potential field from the entire wavefunction [18].

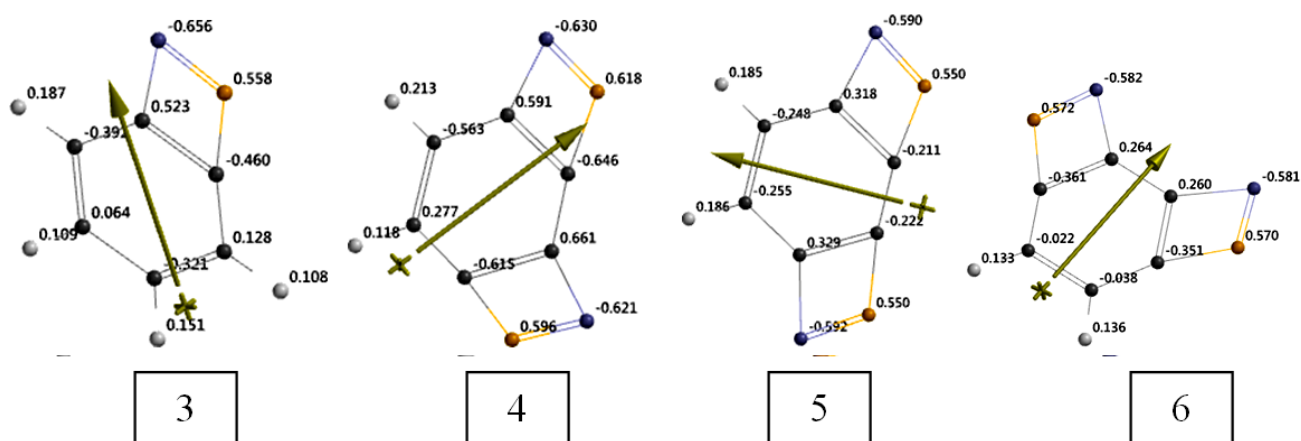


Figure 6. ESP charges on atoms of structures 3-6.

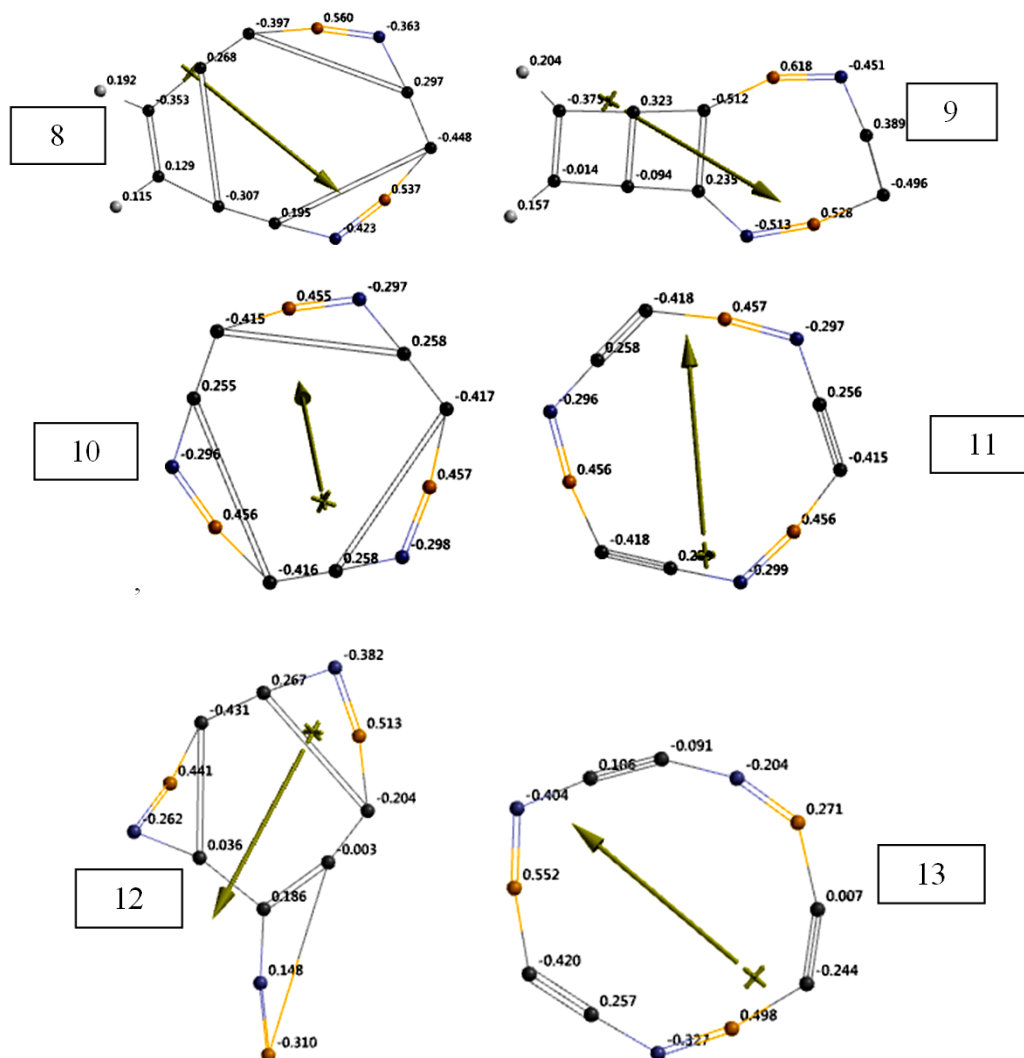
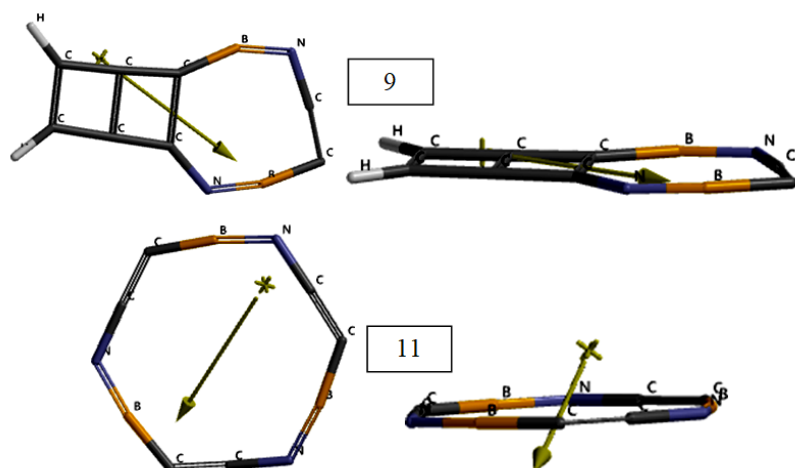


Figure 7. ESP charges on atoms of isomeric structures 8-13.

Figure 8 shows optimized structures 9, 11 and 13 which are isomers of 8, 10 and 12 obtained during the optimization processes. Note that 9, 11 and 13 have one, three and three C-C triple bond(s), respectively. Although structures 11 and 13 are monocyclic systems and in that respect similar to each other, they are different (see below paragraphs).



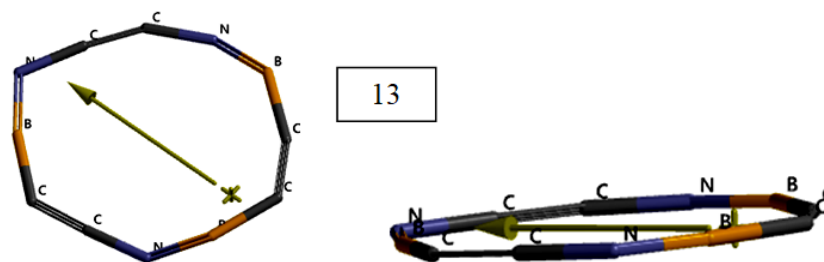
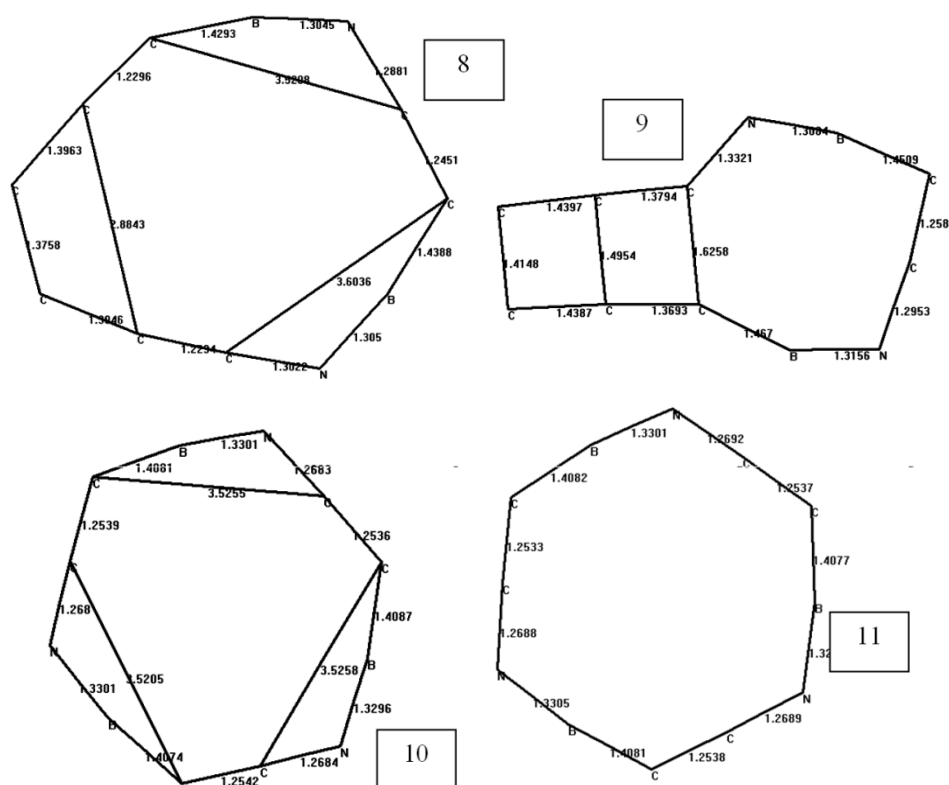


Figure 8. Optimized structures of 9, 11 and 13 (two different views).

Figure 9 displays the calculated bond lengths/ distances (Å) in structures-8 - 13. Note the different long range bonds of 8 with ones in the isomeric structure-10.

Table 1 lists some thermo chemical properties of the species considered. The data in table reveal that the standard heat of formation (H°) values of the species are exothermic and they are favored according to their G° (Gibbs free energy of formation) values. Particular attention should be paid for almost identical thermo chemical properties of isomers-10 and 11. This is not the case for other isomers 8 and 9 and also for 12 and 13. Note that among the isomers 8-13, the order of exothermic character is $10=11>13>12>8>9$. The G values follow the algebraic order of $10=11<13<8<9$. The differences among the isomers should arise from the long range bonds (their numbers, positions and lengths) and the number of 4-membered rings, etc.

Table 2 shows some energies of the species considered. Note that E , ZPE and E_C stand for the total electronic energy, zero point vibrational energy and the corrected total electronic energy, respectively [18]. Again, isomers-10 and 11 exhibit almost identical E , ZPE and E_C values. Similar arguments should be valid for the differences among the E_C values of the isomers. It is noteworthy that although isomer-11 and 13 are monocyclic and having three BN bonds, 11 is more exothermic and more stable than isomer-13. However they differ in terms of fine topology of the heteroatoms.



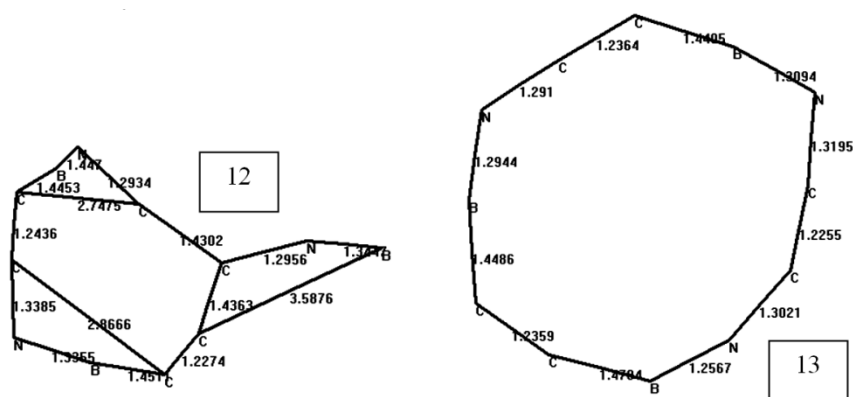


Figure 9. Calculated bond lengths/ distances (Å) in structures 8 - 13.

Table 1. Some thermo chemical properties of the species considered.

Structure	H°	S° (J/mol°)	G°
1	-1209314.411	369.02	-1209424.432
3	-815261.3512	317.45	-815355.999
4	-1020888.538	346.15	-1020991.75
5	-1020848.034	344.93	-1020950.88
6	-1020836.387	347.29	-1020939.93
7	-1215048.311	374.39	-1215159.94
8	-1221152.989	390.17	-1221269.32
9	-1220854.808	375.99	-1220966.91
10	-1227100.916	384.23	-1227215.48
11	-1227100.934	384.22	-1227215.49
12	-1226622.154	391.81	-1226738.97
13	-1226907.758	393.40	-1227025.05

Energies in kJ/mol.

Table 2. Some energies of the species considered.

Structure	E	ZPE	E _C
1	-1209669.20	342.43	-1209326.77
3	-815492.75	221.57	-815271.18
4	-1021079.71	179.57	-1020900.14
5	-1021039.71	180.10	-1020859.61
6	-1021028.05	180.04	-1020848.01
7	-1215335.39	273.99	-1215061.41
8	-1221377.22	209.31	-1221167.91
9	-1221074.88	206.86	-1220868.02
10	-1227262.76	148.18	-1227114.58
11	-1227262.80	148.20	-1227114.60
12	-1226772.98	135.74	-1226637.24
13	-1227067.83	144.69	-1226923.14

Energies in kJ/mol.

Figures 10 and 11 display bond densities of some structures presently considered. Inspection of the data of Figures 10 and 11 reveals that the bond densities are highest around the nitrogen atoms, however they have appreciable values over the 6-membered core for structures 3-6. As for the isomers 8 and 9, the bond density over 4-membered rings of 9 is noticeable. Structures 8-13 have a common appearance that the bond density around the borons are less than the ones about carbons.

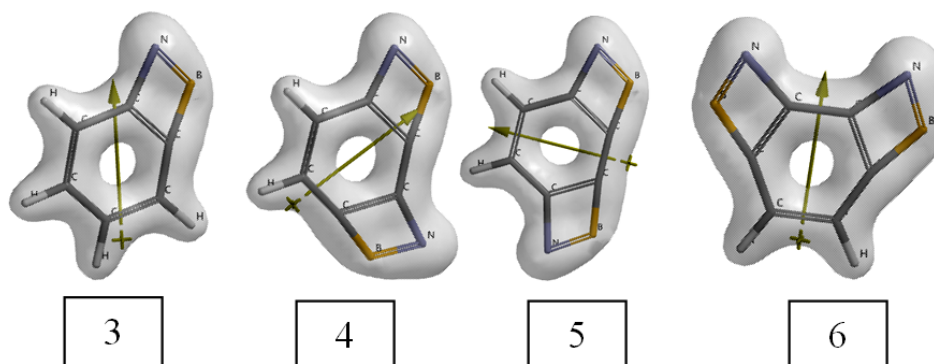


Figure 10. Bond densities of structures 3-6.

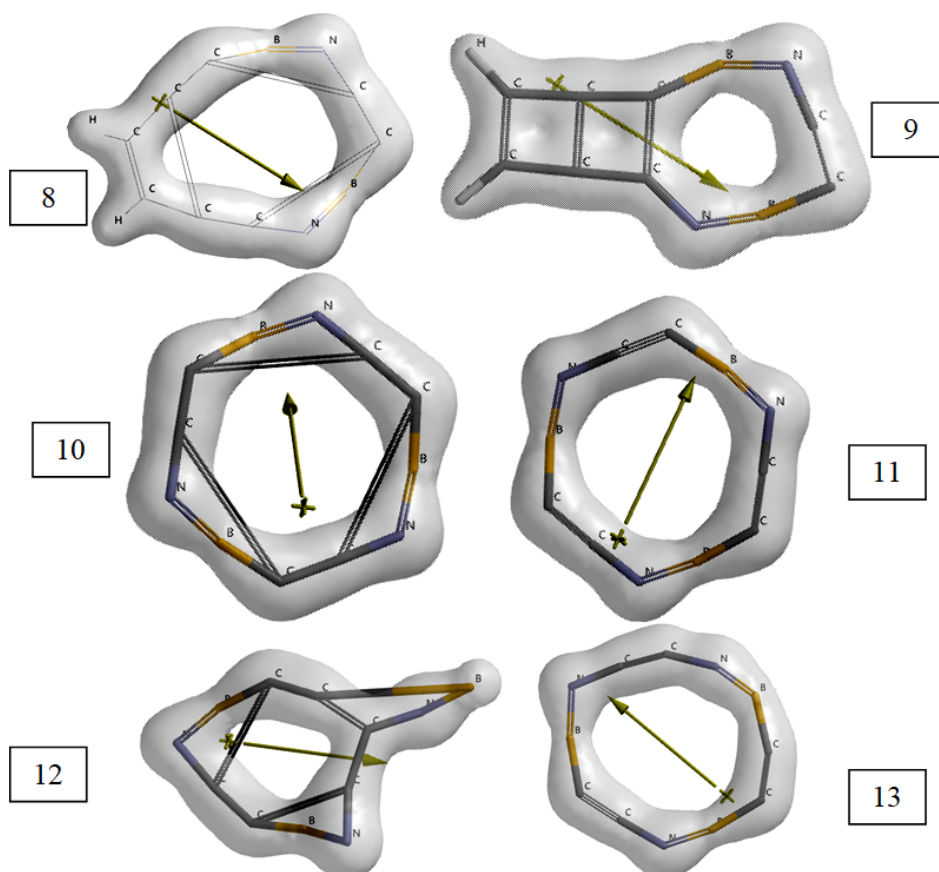


Figure 11. Bond densities of structures 8-13.

Figures 12-14 show some of the molecular orbital energy levels of structures considered. In Figure 12 the most striking fact is regioisomers 4-6 for which the HOMO-NEXTHOMO levels are appreciably affected by the positions/sequences of the boron and nitrogen atoms. Moreover, degeneracy of the LUMO level of structure-6 has to be mentioned.

As seen in Figure 14 structures-10 and 11 possess the identical (almost) molecular orbital energy spectra, thus they are isospectral species in terms of the molecular orbital energy spectra [19-21]. Note that structures-8 and 9 are isomers but not isospectral (similarly 12 and 13).

Structures-11 and 13 are monocyclic and isomers of each other having three BN bonds. However, they are not isospectral. They are originally derived from structures 2 and 2' which are regioisomers and possess different sequence of BN bonds in peripheral circuit.

The HOMO and LUMO energies and the interfrontier molecular orbital gap, $\Delta\epsilon$, values ($\Delta\epsilon = \epsilon_{\text{LUMO}} - \epsilon_{\text{HOMO}}$) of the species considered are listed in Table 3. The algebraic order of HOMO and LUMO energies of the isomers are $10=11 < 12 < 8 < 13 < 9$ and $12 < 13 < 10=11 < 8 < 9$, respectively. Thus, $\Delta\epsilon$ values follow the order of $12 < 13 < 8 < 9 < 10=11$.

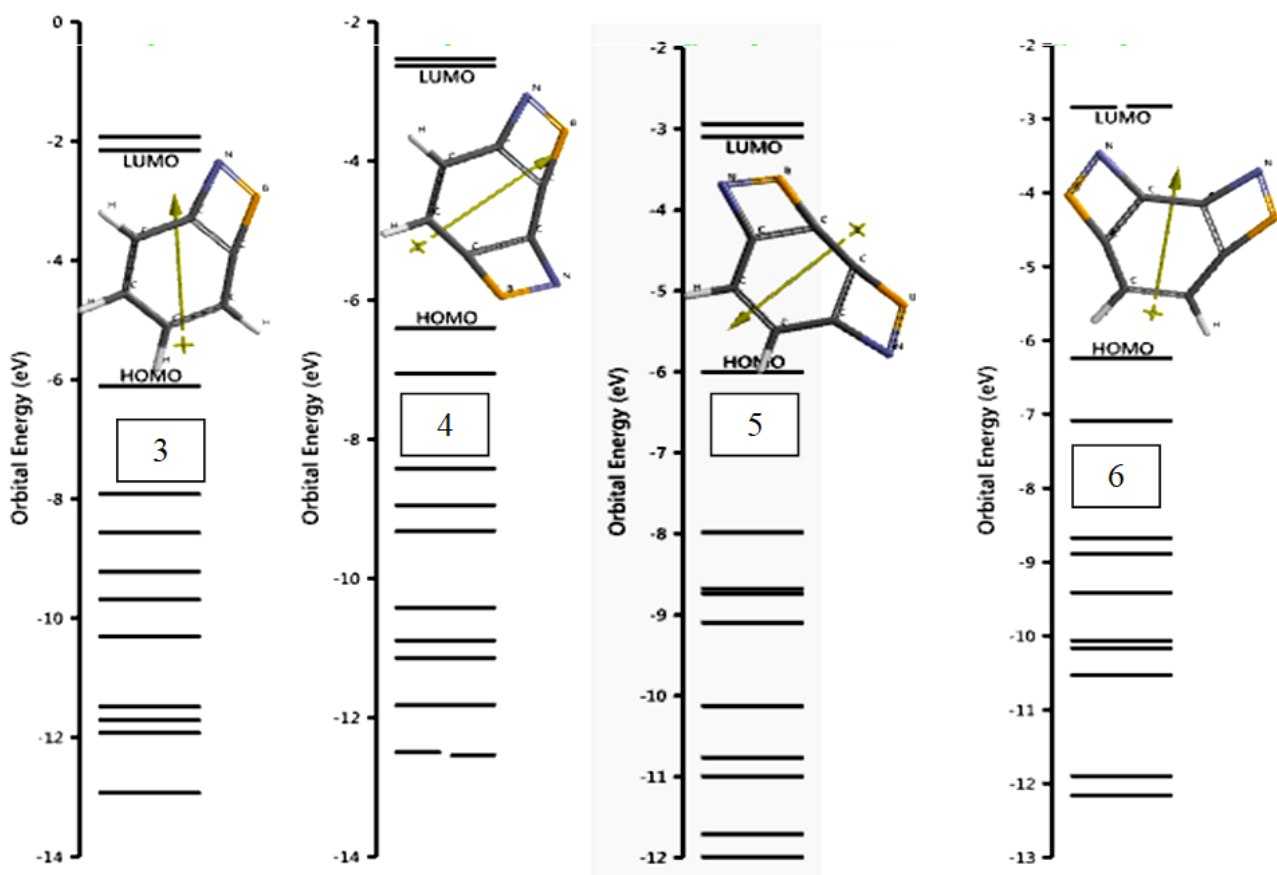


Figure 12. Some of the molecular orbital energy levels of structures 3-6.

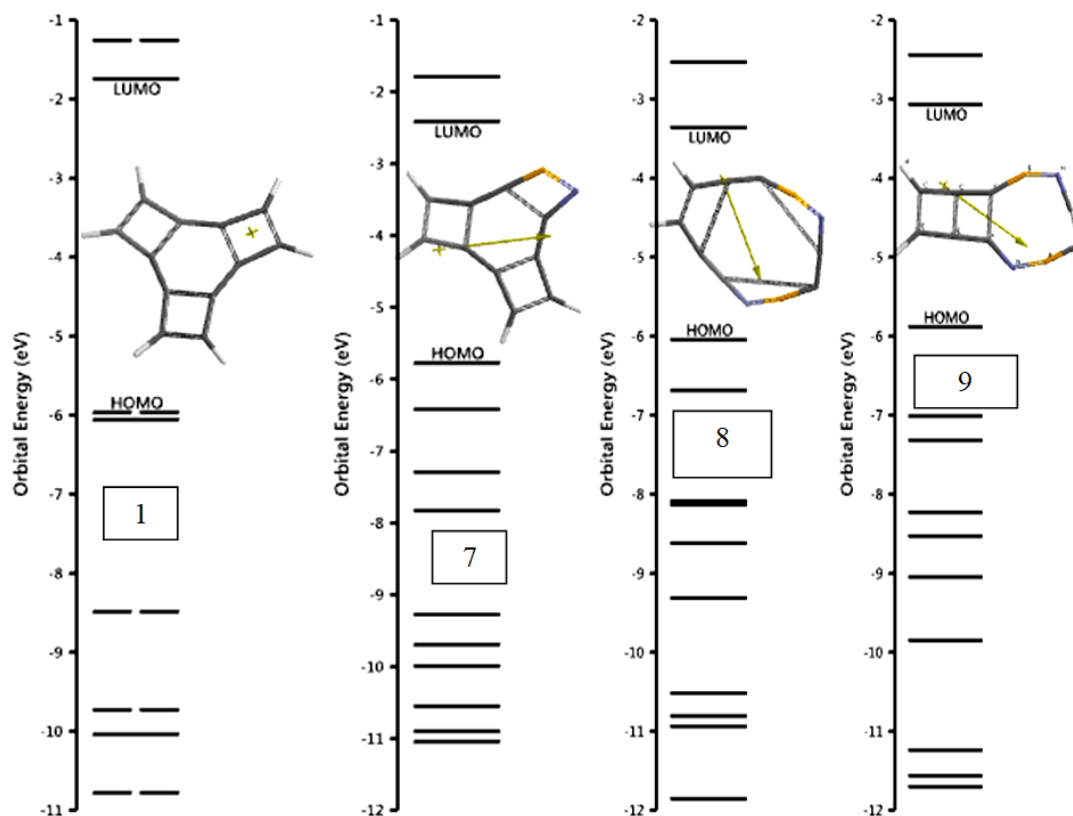


Figure 13. Some of the molecular orbital energy levels of structures 1,7,8 and 10.

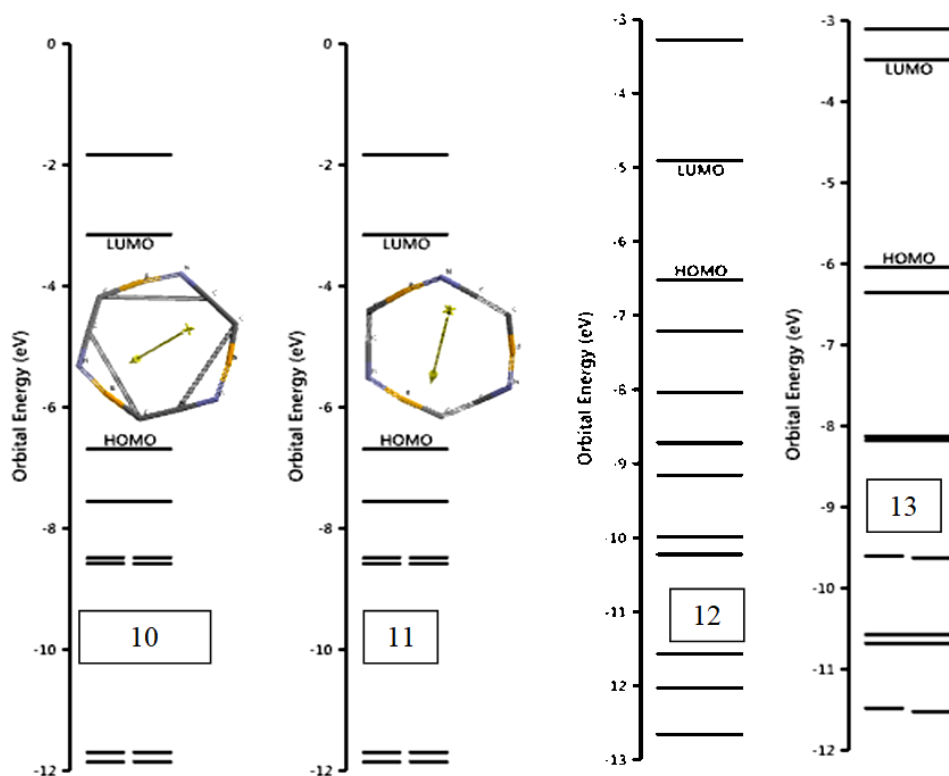


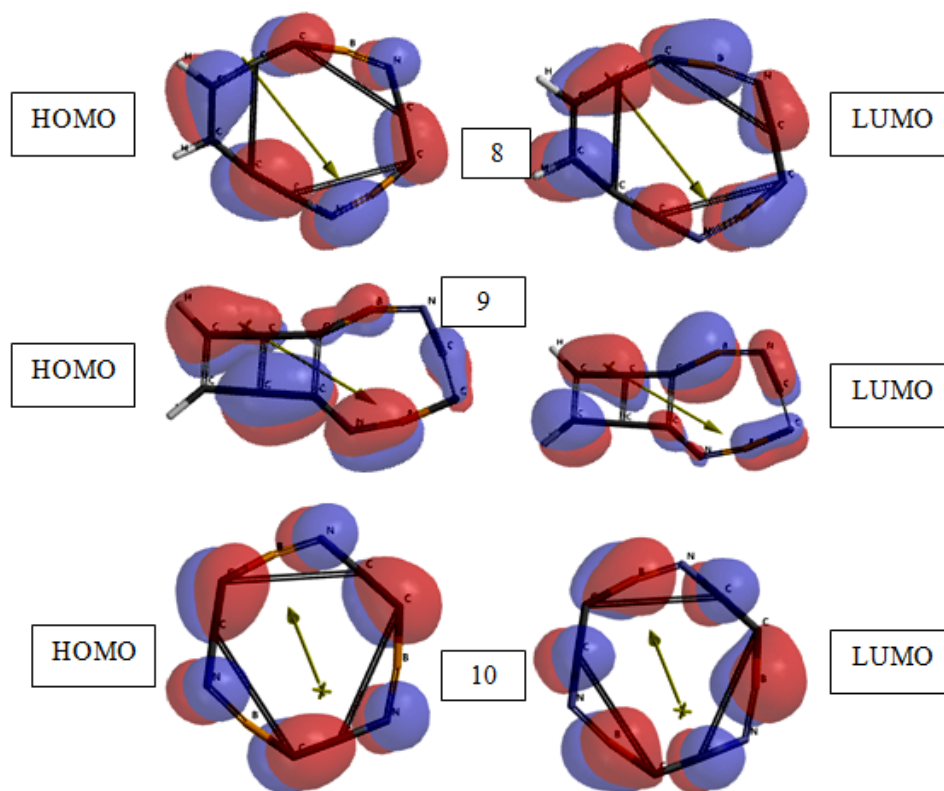
Figure 14. Some of the molecular orbital energy levels of structures 10-13.

Table 3. The HOMO and LUMO energies and $\Delta\varepsilon$ values of the species considered.

Structure	HOMO	LUMO	$\Delta\varepsilon$
1	-575.67	-168.38	380.98
3	-589.09	-208.11	380.98
4	-617.65	-254.26	363.39
5	-579.29	-299.14	280.15
6	-602.25	-273.82	328.43
7	-557.03	-233.07	323.96
8	-583.52	-324.06	259.46
9	-567.90	-296.07	271.83
10	-645.42	-304.06	341.36
11	-645.46	-304.02	341.44
12	-629.22	-473.90	155.32
13	-583.07	-336.10	246.97

Energies in kJ/mol.

Figure 15 shows the HOMO and LUMO patterns of structures 8-13 which are pair wise (8,9; 10,11 and 12,13) related to each other. As seen in the figures a π -symmetry exists in both types of the orbitals. In all the structures the HOMO and LUMO orbitals get participation of all the atoms with few exceptional cases of the boron or nitrogen atoms.



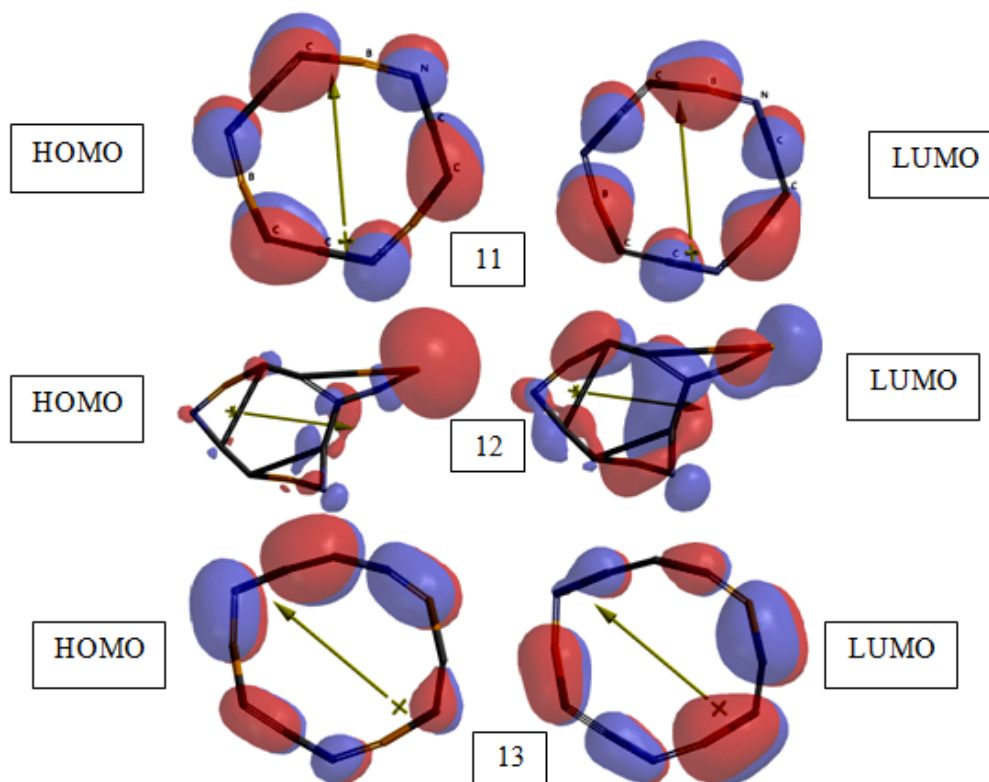


Figure 15. The HOMO LUMO patterns of structures 8-13.

Electrostatic potential maps of species 8-13 are shown in Figure 16 where negative potential regions reside on red/reddish and positive ones on blue/bluish parts of the maps. Note that they are pair wise related to each other.

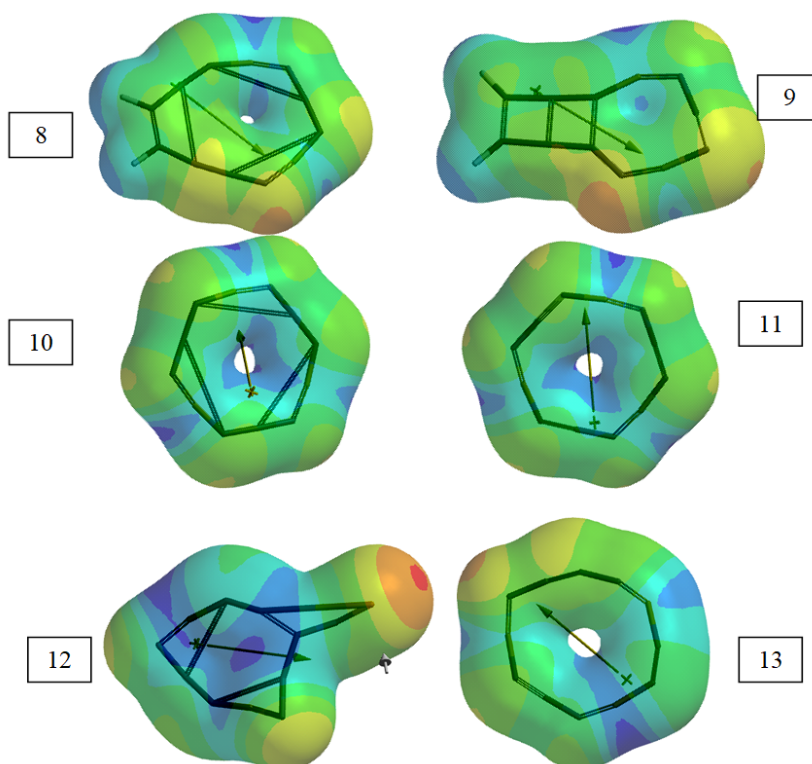


Figure 16. Electrostatic potential maps of species 8-13.

Local ionization potential maps of species 8-13 considered are shown in Figure 17 where conventionally red/reddish regions (if any exists) on the density surface indicate areas from which electron removal is relatively easy, meaning that they are subject to electrophilic attack. Note that the local ionization potential map is a graph of the value of the local ionization potential on an isodensity surface corresponding to a van der Waals surface.

As seen in Figures 16 and 17 the high resemblance between the electrostatic potential (or the local ionization potential) maps of structures-10 and 11 should arise from their isospectral nature.

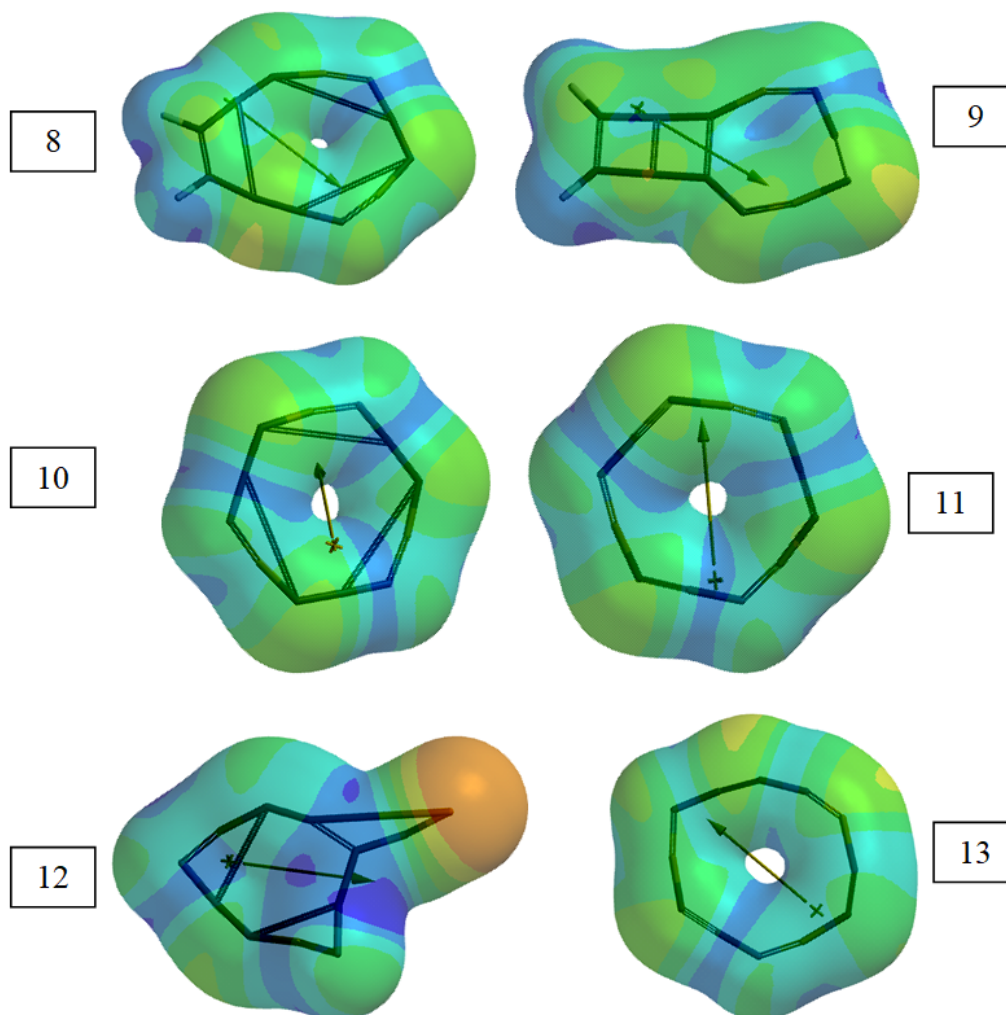
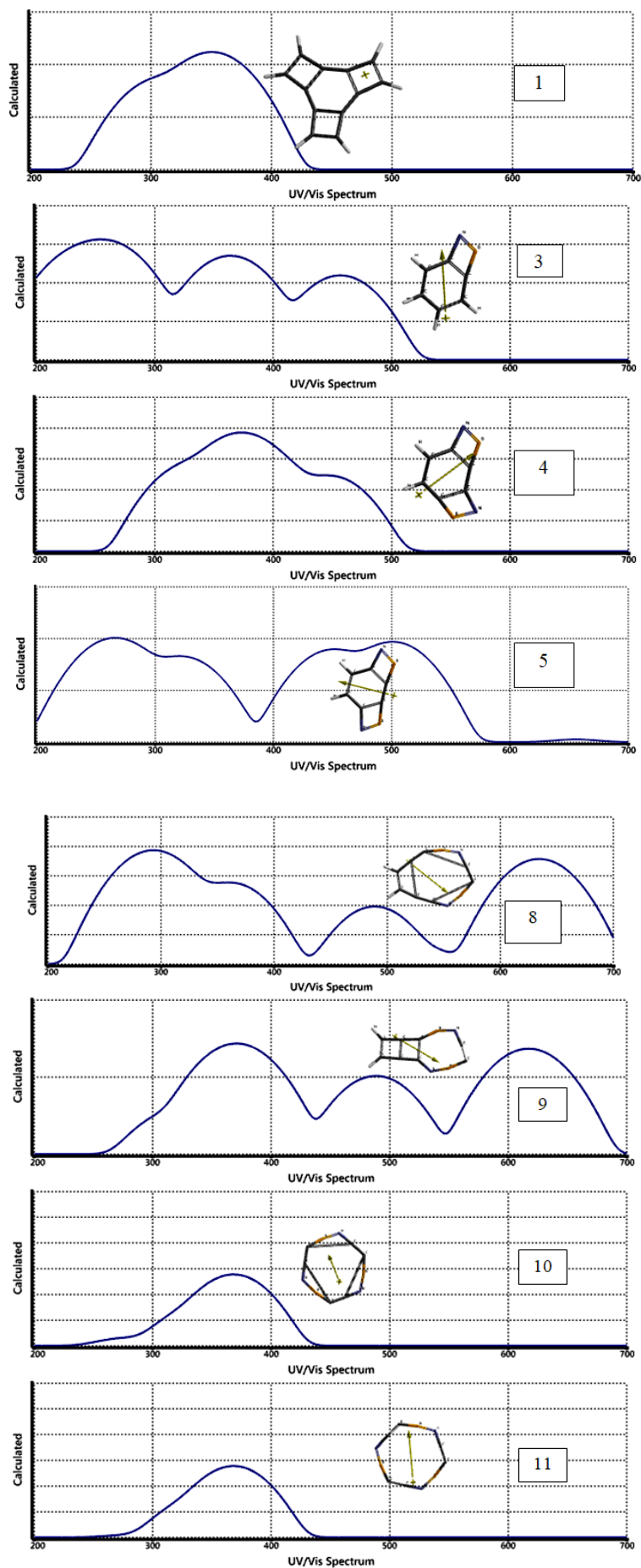


Figure 17. Local ionization potential maps of species 8-13.

Time dependent density functional UV-VIS spectra (TDDFT) of some of the species of interest are shown in Figure 18. The spectrum of compound-1 mainly absorbs in the UV region having λ_{\max} value at 350.60 nm. Insertion of a BN bond spreads the absorption of structure-3 both in the UV and visible regions. Structures-4 and 5 are regioisomers. In spectrum of structure-5 two groups of peaks appear, having shoulders located symmetrically about 400 nm. The isomers-8 and 10 possess similar features except the UV part. Note that the later isomer has a C-C triple bond in the periphery. Structures-10 and 11 exhibit almost the same spectra. As mentioned above they are isospectral structures having the identical molecular orbital energy spectra and are expected to yield the same UV-VIS spectra.

The calculated intensities of the peaks are related to magnitudes of the transition moments between the orbitals involved which vary from isomer to isomer [22,23].



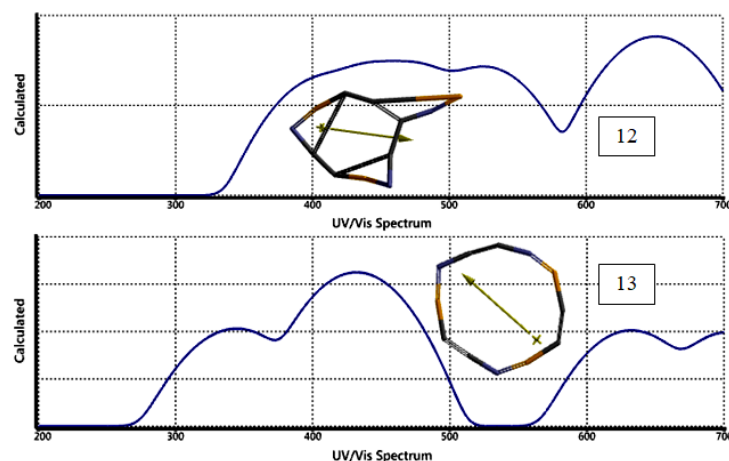


Figure 18. Calculated UV-VIS spectra (TDDFT) of some of the species considered.

4. Conclusion

Various BN-bond containing cyclic structures have been investigated thoroughly within the constraints of density functional theory. They are found to be thermally favored and electronically stable at the standard states. The optimization process in some cases enabled to get more than one isomeric structures of which some are isospectral in terms of the molecular orbital energy spectra. As expected those isospectral isomers produced the identical calculated UV-VIS spectra. Some isomeric structures may exhibit quite different spectra depending on the regioisomers. Some of the optimized structures are monocyclic like annulenes but contain BN bonds in the π -conjugation and are isoconjugate with 12-annulene. Those structures possess two or three C-C triple bonds having the length of 1.20-1.25 Å. Fine topologies governed by the structural and electronic factors arising from the B-N linkage(s) are rather effective.

References

- [1] Dewar, M.J.S., & Dougherty, R.C. (1975). *The PMO theory of organic chemistry*. New York: Plenum/Rosseta.
- [2] Huang, J., & Li, Y. (2018). BN embedded polycyclic π -conjugated systems: Synthesis, optoelectronic properties, and photovoltaic applications. *Frontiers in Chemistry*, 6, 341. <https://doi.org/10.3389/fchem.2018.00341>
- [3] Butenschön, H. (2007). A new oxocarbon $C_{12}O_6$ via highly strained benzyne intermediates. *Angewandte Chemie*, 46 (22), 4012-4014. <https://doi.org/10.1002/anie.200700926>. PMID 17508349.
- [4] Hamura, T., Ibusuki, Y., Uekusa, H., Matsumoto, T., & Suzuki, K. (2006). Poly-oxygenated tricyclobutabenzene via repeated [2 + 2] cycloaddition of benzyne and ketene silyl acetal. *Journal of the American Chemical Society*, 128, 3534-3535. <https://doi.org/10.1021/ja0602647>
- [5] Zachary, X.G., & Shih-Yuan, L. (2018). The state of the art in azaborine chemistry: New synthetic methods and applications. *Journal of the American Chemical Society*, 140(4), 1184-1194. <https://doi.org/10.1021/jacs.7b09446>
- [6] Edel, K., Yang, X., Ishibashi, J.S.A., Lamm, A.N., Maichle-Mössmer, C., Giustra, Z.X., Liu, S.Y., & Bettinger, H.F. (2018). The Dewar isomer of 1,2-dihydro-1,2-azaborinines: isolation, fragmentation, and energy storage. *Angew. Chem. Int. Ed. Engl.*, 57(19), 5296-5300. <https://doi.org/10.1002/anie.201712683>
- [7] Burford, R.J., Li, B., Vasiliu, M., Dixon, D.A., & Liu, S.Y. (2015). Diels-Alder reactions of 1,2-azaborines. *Angew. Chem. Int. Ed. Engl.*, 54(27), 7823-7. <https://doi.org/10.1002/anie.201503483>

- [8] Campbell, P.G., Marwitz, A.J., & Liu, S.Y. (2012). Recent advances in azaborine chemistry. *Angew Chem Int Ed Engl.*, 51(25), 6074-92. <https://doi.org/10.1002/anie.201200063>
- [9] Hirva, P., Turhanen, P., & Timonen, J.M. (2022). Synthesis and theoretical studies of aromatic azaborines. *Organics*, 3(3), 196-209. <http://dx.doi.org/10.3390/org3030016>
- [10] Stewart, J.J.P. (1989). Optimization of parameters for semi-empirical methods I. *J. Comput. Chem.*, 10, 209-220. <https://doi.org/10.1002/jcc.540100208>
- [11] Stewart, J.J.P. (1989). Optimization of parameters for semi-empirical methods II. *J. Comput. Chem.*, 10, 221-264. <https://doi.org/10.1002/jcc.540100209>
- [12] Leach, A.R. (1997). *Molecular modeling*. Essex: Longman.
- [13] Kohn, W., & Sham, L.J. (1965). Self-consistent equations including exchange and correlation effects. *Phys. Rev.*, 140, 1133-1138. <https://doi.org/10.1103/PhysRev.140.A1133>
- [14] Parr, R.G., & Yang, W. (1989). *Density functional theory of atoms and molecules*. London: Oxford University Press.
- [15] Becke, A.D. (1988). Density-functional exchange-energy approximation with correct asymptotic behavior. *Phys. Rev. A*, 38, 3098-3100. <https://doi.org/10.1103/PhysRevA.38.3098>
- [16] Vosko, S.H., Wilk, L., & Nusair, M. (1980). Accurate spin-dependent electron liquid correlation energies for local spin density calculations: a critical analysis. *Can. J. Phys.*, 58, 1200-1211. <https://doi.org/10.1139/p80-159>
- [17] Lee, C., Yang, W., & Parr, R.G. (1988). Development of the Colle-Salvetti correlation energy formula into a functional of the electron density. *Phys. Rev. B*, 37, 785-789. <https://doi.org/10.1103/PhysRevB.37.785>
- [18] SPARTAN 06 (2006). Wavefunction Inc. Irvine CA, USA.
- [19] Graovac, A., Gutman, I., & Trinajstić, N. (1977). *Topological approach to the chemistry of conjugated molecules*. Berlin, Springer-Verlag.
- [20] Türker, L. (1990). An approach to the construction of certain isospectral and subspectral graphs. *MATCH Communications in Mathematical and in Computational Chemistry*, 25, 195-215.
- [21] Türker, L. (2021). Geometrical interpretation of isomers. *Earthline Journal of Chemical Sciences*, 6(2), 155-163. <https://doi.org/10.34198/ejcs.6221.155163>
- [22] Anslyn, E.V., & Dougherty, D.A. (2006). *Modern physical organic chemistry*. Sausalito, California: University Science Books.
- [23] Turro, N.J. (1991). *Modern molecular photochemistry*. Sausalito: University Science Books.

This is an open access article distributed under the terms of the Creative Commons Attribution License (<http://creativecommons.org/licenses/by/4.0/>), which permits unrestricted, use, distribution and reproduction in any medium, or format for any purpose, even commercially provided the work is properly cited.
